October, 1993] © *1993 The Chemical Society of Japan* *Bull. Chem. Soc. Jpn.*, **66**, *2889—2899(1993)* 2889

The Synthesis and X-Ray Crystal Structures of Bis(diethylenetriamine)rhodium(III), Bis(diethylenetriamine)iridium(III), and Bis[bis(3-aminopropyl)amine]rhodium(III) Complexes

Kazumasa Harada
Department of Chemistry, College of Science, Rikkyo (St. Paul's) University, Nishi-ikebukuro 3, Toshima-ku, Tokyo 171

(Received June 25, 1992)

Separations of geometrical isomers of the title complexes were carried out by a column chromatographic method. All three isomers of *mer*-, *sym-fac*-, and *unsym-fac*-$[Rh(dien)_2]^{3+}$ complexes were isolated. The only *mer*-isomer of the $[Ir(dien)_2]^{3+}$ complex was isolated, although trace *fac*-isomers were detected. Although the synthesis of a new $[Rh(dpt)_2]^{3+}$ (dpt=bis(3-aminopropyl)amine) complex was successful, that of $[Ir(dpt)_2]^{3+}$ was not. The only *mer*-$[Rh(dpt)_2]^{3+}$ isomer was obtained. These complexes were characterized by spectroscopic methods. In each case, the obtained *unsym-fac*- and *mer*-isomer were resolved in their antipodes. The crystal structures of three complexes were determined by an X-ray diffraction method. The crystal data are: for *sym-fac*-$[Rh(dien)_2]Br_3$, monoclinic, $C2/c$, $a=14.803(5)$, $b=9.102(3)$, $c=13.989(6)$ Å, $\beta=118.25(3)°$, $Z=4$, $R=0.0478$; for *mer*-$[Rh(dpt)_2]Cl(ClO_4)_2$, monoclinic, $P2_1/a$, $a=18.711(6)$, $b=12.942(5)$, $c=9.714(2)$ Å, $\beta=103.34(3)°$, $Z=4$, $R=0.0275$; for *mer*-$[Ir(dien)_2]$ $(ClO_4)_3\cdot 2H_2O$, orthorhombic, $Aba2$, $a=15.283(9)$, $b=14.736(4)$, $c=10.411(3)$ Å, $Z=4$, $R=0.0341$. The formation ratio of the isomers for the $[Rh(dien)_2]^{3+}$ complex is different from the known ratio for cobalt(III) analogs; this can be attributed to a difference in the M–N bond length based on a molecular mechanics calculation.

Two linear triamines, diethylenetriamine ($NH_2CH_2CH_2NHCH_2CH_2NH_2$, abbreviated as dien) and bis(3-aminopropyl)amine ($NH_2CH_2CH_2CH_2NHCH_2CH_2CH_2NH_2$, abbreviated as dpt), can act as terdentate ligands and coordinate to a central metal ion to form two five- or six-membered chelate rings, respectively. There are two topological coordination modes, *mer* and *fac*. For the bis-type complexes of $[M(dien)_2]^{3+}$ and $[M(dpt)_2]^{3+}$, three geometrical isomers (*sym-fac* (a), *unsym-fac* (b) and (c), and *mer* (d) and (e) isomers) are possible (Fig. 1). The two isomers of *unsym-fac* in Fig. 1 ((b) and (c)) are optical isomers of each other. In *mer*-isomer, an alternative disposition of the N–H bond of the secondary amine in dien or dpt ligands give two structures (Fig. 1 (d) and (e)), which are optical isomers of each other.

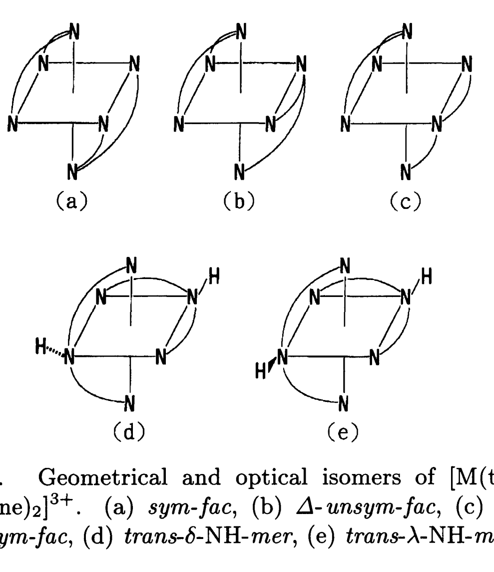

Fig. 1. Geometrical and optical isomers of $[M(triamine)_2]^{3+}$. (a) *sym-fac*, (b) *Δ-unsym-fac*, (c) *Λ-unsym-fac*, (d) *trans-δ*-NH-*mer*, (e) *trans-λ*-NH-*mer*.

The $3d^6$ low-spin N_6-type of cobalt(III) complexes with ammines, which are inert for which it is not necessary to consider the effects of the π electron, have been extensively studied. Nevertheless, there is appreciably limited information available concerning $4d^6$ rhodium(III) or $5d^6$ iridium(III) complexes containing ammines. For example, in $[Co(dien)_2]^{3+}$, many reports have been published concerning the synthesis,[1)] separation and optical resolution of the isomers,[2)] the crystal structures for all of three geometrical isomers,[3—5)] the dependence of the equilibrium isomer proportions on environmental parameter,[6)] and molecular mechanics calculations.[7,8)] On the other hand, Watt and McCormick reported only the synthesis of $[Rh(dien)_2]I_3$ and $[Ir(dien)_2]Br_3$ in their earlier paper,[9)] and did not mention either the separation of isomers or the spectroscopic properties. For $[M(dpt)_2]^{3+}$, a reddish-purple complex, *mer*-$[Co(dpt)_2]^{3+}$, was reported with regard to the synthesis[10,11)] and the crystal structures of racemic *mer*-$[Co(dpt)_2](ClO_4)_3$,[10)] and optically active $(+)^{CD}_{490}$ *mer*-$[Co(dpt)_2]$ $[Co(CN)_6]\cdot 2H_2O$.[12)] The unusual reddish-purple color of these complexes was explained on the basis of the distorted octahedron of chromophore, particularly the extended N–Co–N bond angles, caused by a pair of two-fused six-membered chelate rings in the complex.[11,12)] However, the *fac*-isomers were not obtained. Despite the highly simple system of complexes which have symmetrical linear triamines, there exists a remarkable different stereospecificity of the isomers between complexes having five- and six-membered chelate rings; a few investigations have been reported concerning rhodium(III) or iridium(III) complexes containing these ligands. The difference in the yields of isomers between $[Co(dien)_2]^{3+}$ and $[Co(dpt)_2]^{3+}$ are attributed to the structural characteristics of the two fused fiveor six-membered chelate rings. Six-membered chelate rings give rise to a larger bite size (N···N distance in chelate) than in five-membered rings. In addition, both the conformational flexibility and the structural crowdedness increase in $[M(dpt)_2]^{3+}$ than in $[M(dien)_2]^{3+}$. Although an increase in the flexibility gives an advantage of freedom from a restricted structure, that in the crowdedness leads to a further restriction. The size of the metal ion also influences the structure of the chelate rings. The isomerism in $[M(triamine)_2]^{3+}$ should be greatly affected by these factors, which is specified by not only the constituent numbers in the chelate ring, but also by the size of the metal ion. The change in the metal ion from cobalt(III) to rhodium(III) or iridium(III) in $[M(triamine)_2]^{3+}$ leads us to expect that the construction of complexes in which the difference is only in the size of metal ion, can be approximately attained.

In order to elucidate the effect of the constituent numbers in the chelate ring and/or the size of the metal ion in a complex with triamines, the author reports on the synthesis, spectrochemical properties, and structure of $[M(triamine)_2]^{3+}$ complexes (M=Rh, Ir; triamine=dien, dpt). To interpret the isomerism in terms of the difference in the size of the metal ion, a molecular mechanics calculation involving a variation of the M–N bond length[13] in $[M(dien)_2]^{n+}$ or $[M(dpt)_2]^{n+}$ is also discussed.

Experimental

Synthesis of Complexes. **$[Rh(dien)_2]Cl_3$:** After finely ground $RhCl_3\cdot3H_2O$ (2.0 g) was dissolved in H_2O (3.0 cm^3), dien (3.4 cm^3) was added dropwize to this solution. The solution was then heated in a water bath at 80 °C for 2 h with stirring. After heating, a mixture of dien (2.0 cm^3) and H_2O (0.6 cm^3) was added dropwise to the solution with stirring. Further stirring was continued overnight. Ethanol (400 cm^3) was added to the obtained yellow solution. A powdery pale-yellow precipitate was collected by filtration and washed with ethanol, and air-dried. A crude product was dissolved in a minimum amount of water and, after filtration, white powder of a mixture of geometrical isomers was obtained upon the addition of ethanol to the filtrate. Yield 2.9 g (81%).

Found: C, 20.52; H, 7.01; N, 18.02%. Calcd for $[Rh(dien)_2]Cl_3\cdot3H_2O=RhC_8H_{32}N_6Cl_3O_3$: C, 20.46; H, 6.87; N, 17.89%.

$[Rh(dpt)_2]Cl_3$: Two grams of $RhCl_3\cdot3H_2O$ were dissolved in 4.5 cm^3 H_2O, and 1.0 cm^3 dpt was added dropwise to this solution. The solution was heated in a water bath at 85 °C for 3 h with stirring. Over the period of heating, additional dpt (4.0 cm^3) was added dropwise to the solution. A mixture of ethanol (400 cm^3) and diethyl ether (100 cm^3) was added to the obtained yellow solution; a slightly cream-colored product was precipitated. This was filtered off, dissolved in a small amount of water, and then adsorbed on the top of an SP-Sephadex C-25 column (Na$^+$ form, 3.0$\phi\times$ca. 30 cm). The column was washed with water, followed by hydrochloric acid (0.01 mol dm^{-3}), and then eluted with hydrochloric acid (0.50 mol dm^{-3}). The fractions of which the absorbance at 310 nm was greater than 0.05 were collected. The collected effluent was evaporated on a rotary evaporator to ca. 2 cm^3 at 45 °C. The solution was poured into 400 cm^3 ethanol to obtain a white precipitate. This was filtered off, washed with ethanol, then diethyl ether, and air-dried. Yield 2.8 g (78%).

Found: C, 30.68; H, 7.48; N, 17.61%. Calcd for $[Rh(dpt)_2]Cl_3=RhC_{12}H_{34}N_6Cl_3$: C, 30.56; H, 7.27; N, 17.82%.

$[Ir(dien)_2]Cl_3$: Diethylenetriamine (2.5 cm^3) was carefully added to finely ground $IrCl_3\cdot1.5H_2O$ (1.0 g). This was refluxed for 14 h at 100 °C. During the period of refluxing, additional dien (3.0 cm^3) was added dropwise to the reaction solution. The obtained reddish-brown solution was poured into ethanol (200 cm^3) with stirring. A pale-yellow product was precipitated. This was filtered off and purified by the SP-Sephadex C-25 column chromatographic technique described above (except that the monitored wavelength was 250 nm). A white powder comprising a mixture of geometrical isomers was obtained. Yield 0.70 g (47%).

Found: C, 17.02; H, 5.83; N, 15.26%. Calcd for $[Ir(dien)_2]Cl_3\cdot3H_2O=IrC_8H_{32}N_6Cl_3O_3$: C, 17.19; H, 5.77; N, 15.04%.

Separation and Resolution of Geometrical and Optical Isomers of $[Rh(dien)_2]^{3+}$, $[Ir(dien)_2]^{3+}$, and $[Rh(dpt)_2]^{3+}$. About 0.10 g of each complex salt was adsorbed on the top of an SP-Sephadex column (Na$^+$ form, 2.0$\phi\times$ca. 120 cm), then eluted with a 0.20 mol dm^{-3} Na_2SO_4 solution as an eluent. White powder chloride was obtained from each isomeric band by a similar procedure as that described for purification through SP-Sephadex chromatography. Each geometrical isomer was identified by X-ray analysis for the complex salt crystals of *sym-fac*-$[Rh(dien)_2]^{3+}$, *mer*-$[Ir(dien)_2]^{3+}$, and *mer*-$[Rh(dpt)_2]^{3+}$ and by the chromatographic behavior and spectroscopic properties for others. The isolated geometric isomers and their elemental-analysis data are as follows:

sym-fac-$[Rh(dien)_2]Cl_3\cdot3H_2O$: Found: C, 20.48; H, 6.80; N, 17.76%. Calcd for $RhC_8H_{32}N_6Cl_3O_3$: C, 20.46; H, 6.87; N, 17.89%.

unsym-fac-$[Rh(dien)_2]Cl_3\cdot2.5H_2O$: Found: C, 20.84; H, 6.87; N, 18.05%. Calcd for $RhC_8H_{31}N_6Cl_3O_{2.5}$: C, 20.86; H, 6.78; N, 18.24%.

mer-$[Rh(dien)_2]Cl_3\cdot2.5H_2O$: Found: C, 20.82; H, 6.95; N, 18.25%. Calcd for $RhC_8H_{31}N_6Cl_3O_{2.5}$: C, 20.86; H, 6.78; N, 18.24%.

mer-$[Ir(dien)_2]Cl_3\cdot3H_2O$: Found: C, 17.49; H, 5.93; N, 15.04%. Calcd for $IrC_8H_{32}N_6Cl_3O_3$: C, 17.19; H, 5.77; N, 15.04%.

The optical resolution for each geometric isomer of $[Rh(dien)_2]^{3+}$ and $[Ir(dien)_2]^{3+}$ complexes was carried out through a similar chromatographic procedure, except that a 0.15 mol dm^{-3} sodium bis[(+)$_{589}$-tartrato]diantimonate(III) solution at pH$\fallingdotseq$2, adjusted with hydrochloric acid to avoid racemization and/or decomposition of the complex, was used as the eluent. For the $[Rh(dpt)_2]^{3+}$ complex, the above-mentioned resolution procedure was not effective for a complete resolution of the isomers. The optical resolution of $[Rh(dpt)_2]^{3+}$ was, however, achieved by a recycled column chromatographic method on an SP-Sephadex column (Kiriyama, 2.2$\phi\times$50 cm column). After several cycles, two clearly separated elution bands were obtained.

Preparation of Single Crystals. *sym-fac*-[Rh(dien)]-

Br_3 was obtained from the chloride of the complex by using an SP-Sephadex column with hydrobromic acid as the eluent. Crystals of the complex salt were grown by a vapor-diffusing method (ethanol to aqueous solution of the complex salt); *mer*-[Rh(dpt)$_2$]Cl(ClO$_4$)$_2$ and *mer*-[Ir(dien)$_2$](ClO$_4$)$_3$·2H$_2$O were obtained from each chloride of the complex upon a treatment with perchloric acid. Crystals were grown by a slow evaporation method from an aqueous solution of each complex salt. All of the crystals of the three complex salts were colorless (transparent).

sym-fac-[Rh(dien)$_2$]Br$_3$: Found: C, 17.69; H, 4.95; N, 15.09%. Calcd for $RhC_8H_{26}N_6Br_3$: C, 17.50; H, 4.78; N, 15.31%.

mer-[Rh(dpt)$_2$]Cl(ClO$_4$)$_2$: Found; C, 23.93; H, 5.76; N, 14.12%. Calcd for $RhC_{12}H_{34}N_6Cl_3O_8$: C, 24.03; H, 5.71; N, 14.01%.

mer-[Ir(dien)$_2$](ClO$_4$)$_3$·2H$_2$O: Found; C, 13.45; H, 4.26; N, 11.38%. Calcd for $IrC_8H_{30}N_6Cl_3O_{14}$: C, 13.11; H, 4.13; N, 11.47%.

Spectroscopic Measurements. The ultraviolet absorption spectra, CD spectra and infrared spectra were taken on a Hitachi U-3400 spectrophotometer, a JASCO J-500 spectropolarimeter and a Perkin–Elmer 1600 FTIR spectrometer, respectively. Because all of the present complexes have no characteristic absorption in the visible region, an ADVANTEC UV-750 ultraviolet-monitor was used for the column chromatographic purification or separation of the isomers.

X-Ray Crystal Structure Analysis. The crystal structures of *sym-fac*-[Rh(dien)$_2$]Br$_3$, *mer*-[Rh(dpt)$_2$]Cl(ClO$_4$)$_2$, and *mer*-[Ir(dien)$_2$](ClO$_4$)$_3$·2H$_2$O were determined. Attempts to determine the crystal structures of other isomers failed. The Bragg intensities of their perchlorate salts, both *unsym-fac*- and *mer*-isomers of [Rh(dien)$_2$]$^{3+}$, were rapidly reduced. Data collections were carried out on a Rigaku AFC-5 four-circle diffractometer. Graphite-monochromated Mo $K\alpha$ (λ=0.71073 Å) was used. Corrections for the Lorentz and polarization factors, as well as absorption (North et al.[14]), were employed. The atomic scattering factors for non-hydrogen atoms and hydrogen atoms were taken from Refs. 15 and 16, respectively. The crystal structure of *sym-fac*-[Rh(dien)$_2$]Br$_3$ was determined by a heavy-atom method, and those of *mer*-[Rh(dpt)$_2$]Cl(ClO$_4$)$_2$ and *mer*-[Ir(dien)$_2$](ClO$_4$)$_3$·2H$_2$O by a direct method. The former structure was refined by a block-diagonal least-squares method, and the latter two structures by a full-matrix method. All of the hydrogen atoms were located from a difference synthesis for each complex and included in the refinement. All of the calculation studies were carried out on a FACOM M760/10 computer at the Computer Center of Rikkyo University, using programs of UNICS III,[17] MULTAN,[18] and ORTEP.[19]

Molecular Mechanics Calculation. A molecular mechanics calculation was performed on a FACOM M760/10 computer using the MM2[20] program, which was modified so as to be available for coordination compounds. Except for the case described below, the parameters for the force-field functions in MM2 were chosen from Ref. 8, since they successfully reproduce the structure for ammine complexes of cabalt(III). The total energy was calculated as a function of the M–N bond length so as to evaluated the influence of the M–N bond length on the structure of the complexes. At first, the energy of the input model was minimized with a rather large stretching force constant (30—100 mdyn Å^{-1}, 1dyn=10^{-5} N) for M–N, in order to avoid any concentration of strain to a specific M–N bond. The total energy was then calculated for the minimized structure with normal force constants. The minimization was carried out for the M–N bond length every 0.05 Å for 1.90—2.45 Å (every 0.01 Å around the total energy minimum). The initial molecular geometries were obtained from crystallographic data and/or from calculated data using a molecular processor program called 3D-MOL.[21] To avoid local minima in a calculation with the force field, minimizations from three or more distinct conformations were carried out in the latter case. No formation energy was calculated.

Results and Discussion

Synthesis and Properties of the Complexes. [Rh(dien)$_2$]$^{3+}$: The preparation of [Rh(dien)$_2$]$^{3+}$ and [Ir(dien)$_2$]$^{3+}$ was reported by Watt and McCormick.[9] The present method is a modified version. In the synthesis of [Rh(dien)$_2$]$^{3+}$, they reported that the complex was converted to the iodide for purification. However, the method seems to be inappropriate for efficiently obtaining *fac*-isomers, since the iodides of the *fac*-isomers were more soluble in water than that of the *mer*-isomer. The present purification method is preferred for obtaining the *fac*-isomers.

[Rh(dpt)$_2$]$^{3+}$: A direct synthesis of [Rh(dpt)$_2$]$^{3+}$ from RhCl$_3$·3H$_2$O with dpt in aqueous solution was successfully carried out in satisfactory yield. The preparation of [Co(dpt)$_2$]$^{3+}$ required at least two reaction steps: At first, the unis(dpt) complex was prepared; then the bis(dpt) complex was synthesized.[10,11] A two-step synthesis involving first the formation of a unis(dpt) complex in a methanol or ethanol medium, and then a bis(dpt) complex in an *N,N*-dimethylformamide medium, is also possible. These method, however, do not lead to the formation of *fac*-isomers. Taking into account the yield of the complex and easiness of synthetic operations, the present procedure (described in the Experimental section) seems to be more favorable.

[Ir(dien)$_2$]$^{3+}$: It is well known[22] that the synthesis of iridium(III) complexes containing ammines is not straightforward and that the yields are low. Moreover, it has been reported that the addition of water to the reaction solution would seriously lower the overall yield; this is probably due to the hydrolysis of the starting material in a basic medium.[23] The preparation of [Ir(dien)$_2$]$^{3+}$ was, therefore, carried out in diethylenetriamine (ligand) as a solvent with reference to Watt's method,[9] but using IrCl$_3$·xH$_2$O as a starting material (more available than IrBr$_3$·xH$_2$O). The dropwise mode of the amine is employed to avoid ligand decomposition. The addition of Na$_3$PO$_4$, which was reported to enhance *fac*-isomers formation in [Co(dien)$_2$]$^{3+}$,[6] have also been attempted. In the present case, a relative increase in the formation of *fac*-isomers was observed in the separation of geometrical isomers. This method, however, is less effective for obtaining *fac*-isomers, since the overall yield of the complex is seriously lowered.

An attempt to synthesis $[Ir(dpt)_2]^{3+}$ was unsuccessful. Various solvents, such as bis(3-aminopropyl)amine (ligand), water, dimethyl sulfoxide, *N,N*-dimethylformamide, tetrahydrofuran, methanol, ethanol, and 2-propanol, as well as various starting materials, such as $IrCl_3 \cdot 1.5H_2O$, $IrCl_3$, $Na_2[IrCl_6]$, and $Na_3[IrCl_6]$, have been tried. In the case of methanol and $Na_2[IrCl_6]$, a water-insoluble complex was obtained and confirmed by IR and far-IR spectra to be a dpt- and Cl^--coordinated complex, probably $[IrCl_3(dpt)]$.

Separation of Isomers: The elution curve for the separation of geometrical isomers showed three isomeric elution bands for both the $[Rh(dien)_2]^{3+}$ and $[Ir(dien)_2]^{3+}$ complexes, but only one band for $[Rh(dpt)_2]^{3+}$. For the $[Rh(dien)_2]^{3+}$ complex, all three isomers were isolated from the respective fraction of the elution bands. For the $[Ir(dien)_2]^{3+}$ complex, however, the isomers corresponding to the first and second elution bands could not be isolated, because of their extremely low yields. The configurations of the isomers were assigned on the basis of the elution order compared with that of the $[Co(dien)_2]^{3+}$ complex.2) The order is *sym-fac*, *unsym-fac*, and then *mer*. The configurations of *sym-fac*-$[Rh(dien)_2]^{3+}$ and *mer*-$[Ir(dien)_2]^{3+}$ isomers were confirmed by X-ray analysis for the crystal of each complex salt. Only one isomer of $[Rh(dpt)_3]^{2+}$ obtained was assigned to the *mer*-isomer by X-ray analysis. All of the isomers assigned to *unsym-fac* or *mer* in each complex were divided into enantiomeric pairs by the optical-resolution procedure mentioned above; the isomers assigned to *sym-fac*, however, were not. These results support the validity of the assignment for *sym-fac*- and *unsym-fac*-$[Ir(dien)_2]^{3+}$ isomers which could not be isolated as complex salts. The absolute configurations of the optical isomers were assigned on the basis of the elution order on optical resolution compared with that of corresponding cobalt(III) complexes, of which absolute configurations have been determined.4,5,12) That is, the absolute configurations of the isomer for the former elution band in the optical resolution are assigned to *Λ-unsym-fac*-$[M(dien)_2]^{3+}$ (Fig. 1(c)) and *trans*-λ-NH-*mer*-$[M(dien)_2]^{3+}$ (M=Rh, Ir; Fig. 1(e)), and *trans*-δ-NH-*mer*-$[Rh(dpt)_2]^{3+}$ (Fig. 1(d)), respectively.

Ultraviolet (UV), Circular Dichroism (CD), and Infrared (IR) Spectra: The UV absorption spectra and CD spectra are shown in Figs. 2, 3, and 4; the numerical data are summarized in Table 1 with the corresponding cobalt(III) complexes, in which the ligand field assignments in the O_h effective site symmetry are included. It is clear from Figs. 2, 3, and 4 and Table 1 that the UV-visible absorption spectra in the system of $[M(triamine)_2]^{3+}$ show a good correspondence, considering the differences in the ligand field strength among the cobalt(III), rhodium(III), and iridium(III) complexes. It is well known that the spectrochemical series for the three kinds of metal ions is: cobalt(III) < rhodium(III) < iridium(III).25—28) As shown in Fig. 4, the absorption band of *mer*-$[Ir(dien)_2]^{3+}$ had a shoulder at ca. 31×10^3 cm^{-1}. This can be assigned to the $^3T_{1g} \leftarrow {}^1A_{1g}$ spin-forbidden transition, suggesting a significant spin-orbit coupling for the $5d^6$ iridium(III) com-

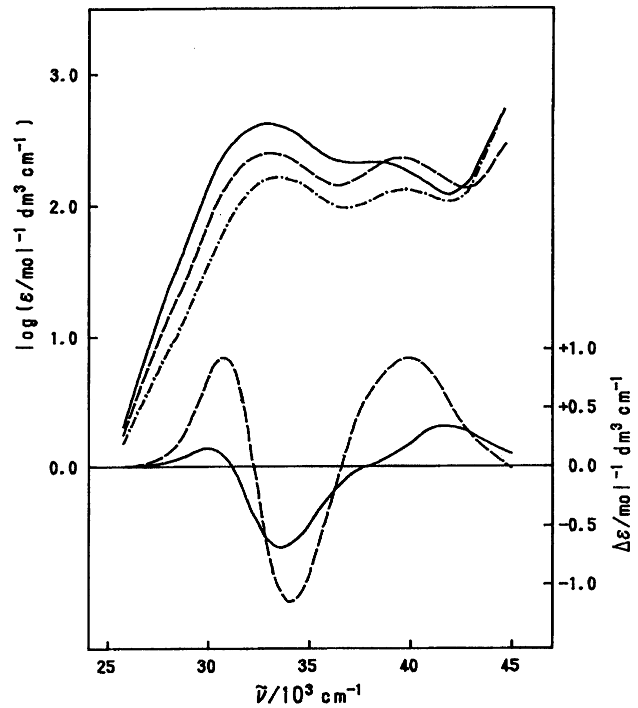

Fig. 2. Absorption and CD spectra of $[Rh(dien)_2]^{3+}$. —•—: *sym-fac*-, ---: *unsym-fac*-, ——: *mer*-isomer.

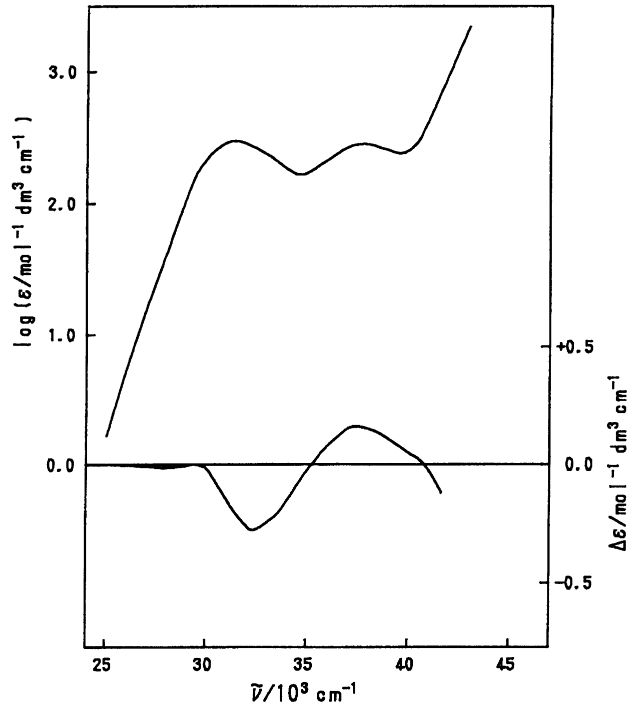

Fig. 3. Absorption and CD spectrum of *mer*-$[Ir(dien)_2]^{3+}$.

Table 1. Absorption Maxima and CD Peaks[a)] of Some $[M(triamine)_2]^{3+}$ Complexes

Complex	$^1T_{1g}\leftarrow{}^1A_{1g}$		$^1T_{2g}\leftarrow{}^1A_{1g}$					
	$\tilde{\nu}/10^3$ cm^{-1} (ε/mol^{-1} dm^3 cm^{-1})				$\tilde{\nu}/10^3$ cm^{-1} ($\Delta\varepsilon$/mol^{-1} dm^3 cm^{-1})			
$[Co(dien)_2]^{3+}$ b)								
sym-fac-	21.8	(66.5)	30.0	(61.5)				
unsym-fac-	21.5	(93.0)	29.7	(88.5)	19.9	(+0.98)	22.5	(−0.84)
mer-	21.6	(146)	29.3	(107)	19.5	(+0.096)	21.9	(−0.181)
$[Rh(dien)_2]^{3+}$								
sym-fac-	33.4	(163)	40.1	(130)				
unsym-fac-	32.9	(248)	39.6	(222)	30.8	(+0.93)	34.1	(−1.16)
mer-	33.1	(419)	38.5	(210)	29.5	(+0.160)	33.1	(−0.691)
$[Ir(dien)_2]^{3+}$								
sym-fac- c)	40.2	(—)						
unsym-fac- c)	39.5	(—)			35.7	(+)	39.7	(−)
mer-	39.8	(315)			31.9	(+0.13)	38.9	(−0.58)
$[Co(dpt)_2]^{3+}$								
mer-	19.4	(93.3)	27.2	(97.7)	18.2	(+0.110)	20.4	(−0.130)
$[Rh(dpt)_2]^{3+}$								
mer-	31.5	(302)	37.7	(282)	31.5	(−0.015)	32.5	(−0.285)

a) First absorption region ($^1T_{1g}\leftarrow{}^1A_{1g}$) of Λ-isomer for *unsym-fac* and *trans*-λ-NH-isomer for *mer*. b) Ref. 2. c) These absorption coefficients have not been determined.

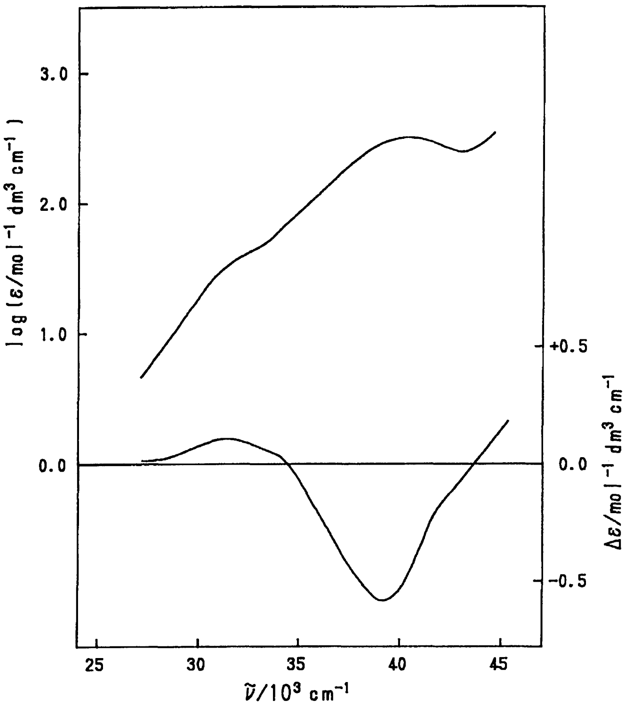

Fig. 4. Absorption and CD spectrum of *mer*-$[Rh(dpt)_2]^{3+}$.

plex, compared with the $3d^6$ cobalt(III) or $4d^6$ rhodium(III) complex.[24)] In $[M(dpt)_2]^{3+}$ complexes, which have a pair of two-fused six-membered chelate rings, the absorption maxima in the first d–d transition region are shifted to a lower energy side than that in the corresponding dien complexes, which have a pair of two-fused five-membered chelate rings. It shows good agreement with the general tendency that the ligand field strength is lowered when the five-membered ring is replaced by a six-membered one in the polyamine chelate.[11)] However, regarding the difference in the wavenumber of the first ligand field absorption maxima between the *mer*-$[M(dien)_2]^{3+}$ and *mer*-$[M(dpt)_2]^{3+}$ complex, it is worth remarking that the difference is lowered in the rhodium(III) complexes than that in the cobalt(III) complexes. This suggests that the distortion of the octahedron chromophore in the *mer*-$[Rh(dpt)_2]^{3+}$ complex is more relaxed than that in the *mer*-$[Co(dpt)_2]^{3+}$ complex.

For optically active isomers, both the spectra and the numerical data are shown for only the Λ-isomer of *unsym-fac*-$[M(dien)_2]^{3+}$, *trans*-λ-NH-isomer[5)] of *mer*-$[M(dien)_2]^{3+}$ and of *mer*-$[Rh(dpt)_2]^{3+}$ complexes, since the respective antipodes indicated quite symmetrical CD patterns. All of the CD spectra in the first absorption band region shown a negative main peak in the higher energy side and a positive one in the lower energy side, except in *mer*-$[Rh(dpt)_2]^{3+}$. The latter case, however, also has a negative main peak at the higher energy side, and the $\Delta\varepsilon$ value of the negative peak at the lower energy side (ca. 28×10^3 cm^{-1}) is very low. The $\Delta\varepsilon$ values of *mer*-type complexes were relatively low, compared with the *unsym-fac* ones. This is because in the *mer*-type complex the chirality depends only on the contribution of *trans*-NH (mutual orientation between H atoms bonding to the respective two secondary amine N atoms).

The IR spectra of the present rhodium(III) and iridium(III) complexes were very similar to the corresponding cobalt(III) complexes.[2,11)] Schmidtke and Garthoff[29)] reported on details concerning the IR spectra of $[MX_3(dien)]$ (M = Rh, Cr, Co, Mo), and Yoshikawa et al.[2)] reported that three isomers (*sym-fac*-, *unsym-fac*-, and *mer*-$[Co(dien)_2]^{3+}$) are distinguishable based on the IR spectra using Schmidtke's results. The

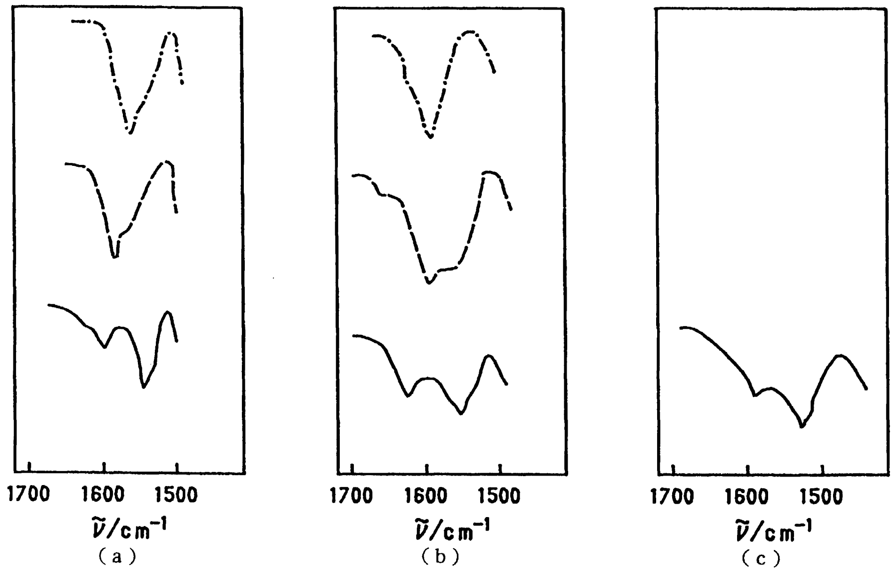

Fig. 5. Infrared spectra of $[M(dien)_2]Cl_3$. a: M=Co, b: M=Rh, c: M=Ir. —•—: *sym-fac-*, - - -: *unsym-fac-*, —: *mer-*isomer.

Table 2. Summary of X-Ray Data Collections, Crystal Data, and Structure Refinements

	sym-fac-$[Rh(dien)_2]Br_3$	*mer-*$[Rh(dpt)_2]Cl(ClO_4)_2$	*mer-*$[Ir(dien)_2](ClO_4)_3 \cdot 2H_2O$
Formula	$RhC_8H_{26}N_6Br_3$	$RhC_{12}H_{34}N_6O_8Cl_3$	$IrC_8H_{30}N_6O_{14}Cl_3$
F.W.	548.95	599.70	732.94
Crystal system	Monoclinic	Monoclinic	Orthorhombic
Space group	$C2/c$	$P2_1/a$	$Aba2$
a/Å	14.803(5)	18.711(6)	15.283(9)
b/Å	9.102(3)	12.942(5)	14.736(4)
c/Å	13.989(6)	9.714(2)	10.411(3)
β/°	118.25(3)	103.34(3)	
V/Å^3	1660.4(11)	2288.8(13)	2344.6(16)
Z	4	4	4
D_c/g cm^{-3}	2.20	1.74	2.08
D_m/g cm^{-3}	2.19	1.74	2.06
μ (Mo $K\alpha$)/cm^{-1}	20.4	11.3	60.9
Crystal habit	Column	Polyhedral	Plate
Crystal size/mm	0.2×0.15×0.35	0.15×0.15×0.15	0.2×0.3×0.15
Scan mode (range)	ω $(2\theta \leq 25°)$ ω–2θ $(25° < 2\theta \leq 55°)$	ω–2θ $(2\theta \leq 55°)$	ω–2θ $(2\theta \leq 55°)$
Scan width/°	$1.25+0.60\tan\theta$	$1.10+0.45\tan\theta$	$1.00+0.45\tan\theta$
Scan speed/° min^{-1}	4	4	2
No. of unique refl. with $F_o \geq 3\sigma(F_o)$	1606	3781	1750
Max. min. residual elctron density/eÅ^{-3}	0.943, −2.116	0.726, −0.800	1.519, −1.168
Max. (shift/esd)	0.23	0.08	0.04
$R^{a)}$	0.0478	0.0275	0.0341
$R'^{b)}$	0.0644	0.0292	0.0391

a) $R=(\Sigma||F_o(h)|-|F_c(h)||)/(\Sigma|F_o(h)|)$. b) $R'=((\Sigma(|F_o(h)|-|F_c(h)|)^2)/(\Sigma|F_o(h)|^2))^{1/2}$.

region at about 1600 cm^{-1} (δ–NH_2) of the spectra is very clear for distinguishing the isomers; that is, the *sym-fac*-isomer has a single peak, the *unsym-fac* one a single peak with a shoulder, and the *mer* one two splitting peaks. The IR spectra of $[M(dien)_2]Cl_3$ complexes in this region are shown in Fig. 5. It reveals that the assignment of the isomers can be reasonably applied to the present complexes.

Structures. Experimental details, crystallographic data and the R factors of the final refinements are given in Table 2. The atomic and thermal parameters of the complexes are given in Tables 3, 4, and 5. Perspective

Table 3. Final Atomic Coordinates ($\times10^4$) and Their Equivalent Isotropic Thermal Parameters of *sym-fac*-$[\mathrm{Rh(dien)_2}]\mathrm{Br_3}$

Atom	x/a	y/b	z/c	$B_{eq}/\text{Å}^2$ a)
Rh	2500	2500	5000	1.3
Br(1)	0	119(4)	2500	3.8
Br(2)	1136(1)	3544(2)	1316(1)	2.5
N(1)	1252(9)	3743(15)	3935(10)	2.2
N(2)	3290(9)	4350(13)	4937(9)	1.9
N(3)	2764(9)	1826(13)	3741(9)	1.9
C(1)	1529(15)	5312(19)	3918(14)	3.3
C(2)	2618(16)	5651(18)	4781(16)	3.6
C(3)	3542(15)	4258(20)	4052(16)	3.6
C(4)	3646(12)	2683(19)	3781(14)	2.8

a) $B_{\mathrm{eq}}=4/3(\sum_i\sum_j B_{ij}\,\boldsymbol{a}_i\cdot\boldsymbol{a}_j)$.

Table 4. Final Atomic Coordinates ($\times10^4$) and Their Equivalent Isotropic Thermal Parameters of *mer*-$[\mathrm{Rh(dpt)_2}]\mathrm{Cl(ClO_4)_2}$

Atom	x/a	y/b	z/c	$B_{eq}/\text{Å}^2$ a)
Rh	3443.4(2)	2141.2(2)	2611.2(3)	1.9
Cl(1)	1395.3(6)	3029.1(8)	5659.6(11)	3.4
Cl(2)	4244.4(7)	3475.5(9)	8075.8(11)	4.0
Cl(3)	1830.1(6)	4524.8(9)	928.0(12)	4.0
O(1)	745(2)	3646(3)	5382(4)	5.6
O(2)	1845(3)	3389(4)	6965(4)	7.8
O(3)	1205(3)	1987(3)	5685(6)	9.2
O(4)	1770(2)	3219(3)	4564(4)	5.8
O(5)	3903(3)	3757(3)	6676(4)	8.4
O(6)	3821(3)	2749(4)	8581(4)	8.5
O(7)	4397(3)	4349(4)	8961(4)	8.2
O(8)	4913(3)	2980(5)	8064(7)	11.3
N(1)	3683(2)	649(3)	2037(4)	2.7
N(2)	4323(2)	2772(3)	1846(4)	2.8
N(3)	3115(2)	3584(3)	3264(4)	2.7
N(4)	4146(2)	2009(3)	4611(3)	2.8
N(5)	2534(2)	1516(3)	3289(4)	2.7
N(6)	2784(2)	2426(3)	572(4)	3.1
C(1)	4454(2)	341(4)	2112(5)	3.2
C(2)	4802(3)	1036(4)	1227(5)	3.8
C(3)	4972(2)	2098(4)	1828(5)	3.6
C(4)	4604(3)	3810(4)	2404(5)	3.5
C(5)	4008(3)	4614(4)	2289(5)	3.7
C(6)	3583(3)	4525(4)	3419(5)	3.4
C(7)	4027(3)	1183(4)	5604(5)	3.6
C(8)	3252(3)	1192(4)	5797(5)	4.0
C(9)	2690(3)	808(4)	4541(5)	3.7
C(10)	1948(3)	1004(4)	2182(5)	3.6
C(11)	1633(2)	1659(4)	912(5)	3.8
C(12)	2137(2)	1779(4)	−75(5)	3.5

a) $B_{\mathrm{eq}}=4/3(\sum_i\sum_j B_{ij}\,\boldsymbol{a}_i\cdot\boldsymbol{a}_j)$.

drawings of the complex cations are shown in Figs. 6, 7, and 8. Tables of anisotropic thermal parameters for non-hydrogen atoms, parameters of hydrogen atoms, as well as the observed and calculated structure factors are deposited as Document No. 66041 at the office of the Editor of Bull. Chem. Soc. Jpn.

Table 5. Final Atomic Coordinates ($\times10^3$) and Their Equivalent Isotropic Thermal Parameters of *mer*-$[\mathrm{Ir(dien)_2}](\mathrm{ClO_4})_3\cdot2\mathrm{H_2O}$

Atom	x/a	y/b	z/c	$B_{eq}/\text{Å}^2$ a)
Ir	500	500	0	2.1
Cl(1)	500	1000	6(7)	5.4
Cl(2)	830(1)	752(1)	185(1)	4.7
O(1)	492(3)	1075(2)	83(2)	8.8
O(2)	567(2)	985(3)	−78(4)	13.7
O(3)	838(3)	837(2)	235(4)	9.5
O(4)	919(2)	727(2)	154(4)	9.8
O(5)	799(2)	690(3)	279(4)	13.0
O(6)	780(2)	750(3)	75(3)	11.6
O(W)	588(1)	756(1)	13(4)	5.9
N(1)	539(2)	596(3)	148(3)	4.0
N(2)	629(1)	464(1)	15(4)	3.3
N(3)	493(3)	401(2)	−134(3)	3.8
C(1)	638(2)	574(2)	175(4)	4.3
C(2)	678(2)	543(2)	60(3)	4.6
C(3)	651(3)	429(3)	−130(4)	7.0
C(4)	585(2)	364(3)	−157(3)	4.9

a) $B_{\mathrm{eq}}=4/3(\sum_i\sum_j B_{ij}\,\boldsymbol{a}_i\cdot\boldsymbol{a}_j)$.

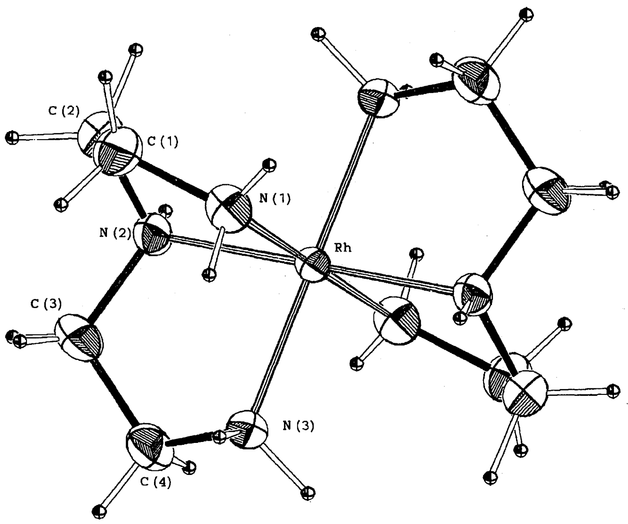

Fig. 6. Perspective drawing of the *sym-fac*-$[\mathrm{Rh(dien)_2}]^{3+}$ cation.

***sym-fac*-$[\mathbf{Rh(dien)_2}]\mathbf{Br_3}$:** Figure 6 shows that the complex has a *sym-fac* configuration with six nitrogen atoms forming an octahedral complex. Since a rhodium atom occupies a special position of $\bar{1}$ in the space group $C2/c$, the complex cation, itself, has an inversion symmetry. Although a pair of two-fused five-membered chelate rings have a ($\delta\delta$, $\lambda\lambda$) conformation, in contrast to *sym-fac*-$[\mathrm{Co(dien)_2}]\mathrm{Br_3}$, which has ($\delta\lambda$, $\lambda\delta$) conformation,[3] the same ($\delta\delta$,$\lambda\lambda$) conformation was reported for $(-)_{589}$-*unsym-fac*-$[\mathrm{Co(dien)_2}][\mathrm{Co(CN)_6}]\cdot2\mathrm{H_2O}$.[4] The bond lengths and angles are listed in Table 6, and are consistent with those for known rhodium(III) complexes containing ammines.[30,31]

***mer*-$[\mathbf{Rh(dpt)_2}]\mathbf{Cl(ClO_4)_2}$:** As shown in Fig. 7,

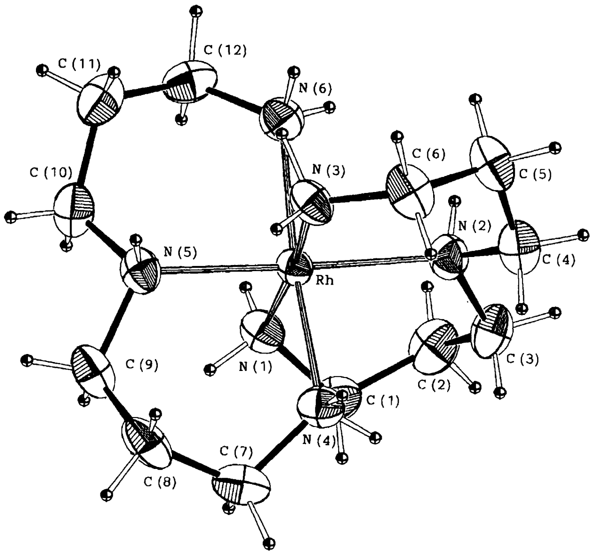

Fig. 7. Perspective drawing of the *mer*-$[Rh(dpt)_2]^{3+}$ cation.

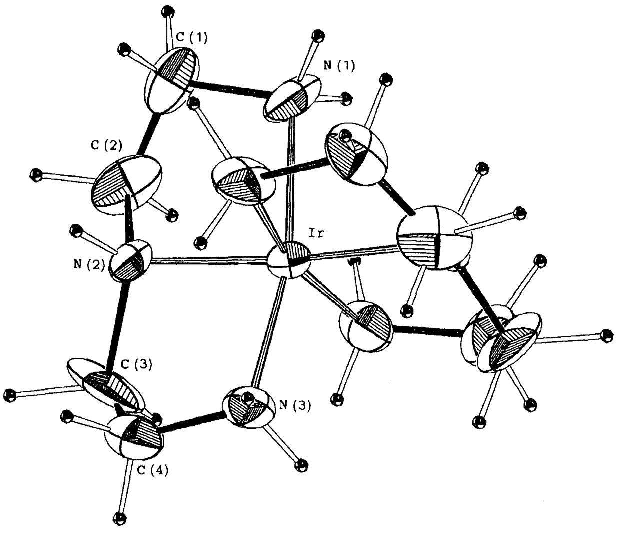

Fig. 8. Perspective drawing of the *mer*-$[Ir(dien)_2]^{3+}$ cation.

Table 6. Bond Distances and Angles within *sym-fac*-$[Rh(dien)_2]^{3+}$

Bond distance	l/Å	Bond angle	ϕ/°
Rh–N(1)	2.075(13)	N(1)–Rh–N(2)	81.7(5)
Rh–N(2)	2.075(13)	N(1)–Rh–N(3)	90.8(5)
Rh–N(3)	2.070(13)	N(2)–Rh–N(3)	82.4(5)
N(1)–C(1)	1.49(3)	Rh–N(1)–C(1)	112.1(11)
N(2)–C(2)	1.45(3)	Rh–N(2)–C(2)	107.5(12)
N(2)–C(3)	1.46(3)	Rh–N(2)–C(3)	111.5(12)
N(3)–C(4)	1.50(2)	Rh–N(3)–C(4)	109.0(10)
C(1)–C(2)	1.52(3)	C(2)–N(2)–C(3)	110.0(15)
C(3)–C(4)	1.51(3)	N(1)–C(1)–C(2)	112.2(17)
		N(2)–C(2)–C(1)	109.7(18)
		N(2)–C(3)–C(4)	111.5(17)
		N(3)–C(4)–C(3)	108.2(15)

two dpt ligands coordinate to a rhodium atom with six nitrogen atoms to form an octahedral complex. Each ligand occupies a meridional position. A pair of two-fused six-membered chelate rings adopt an all-chair conformation. Since the rhodium atom lies at a general position, there exist two enantiomeric pairs of the complex cation in a unit cell. One of them has a *trans*-λ-NH absolute configuration (Fig. 7), and the other has a *trans*-δ-NH configuration. The bond length and angles in the complex cation are listed in Table 7. The Rh–N bond lengths (2.122(4) and 2.087(4) Å) agreed with the values observed in *mer*-$[RhCl(dpt)(NN)]^{3+}$ (NN=bpy or phen)[32] and *trans*-$[Rh(CN)_2(tn)_2]^{+}$[33] complexes containing six-membered chelate rings. All of the chelate angles of N(terminal)–Rh–N(secondary) in the dpt chelates are larger than 90°. These results indicate that the six-membered chelate rings are considerably extended to open N–Rh–N angles. Such a tendency was also observed in the *mer*-$[Co(dpt)_2]^{3+}$ complex.[10,12] However, the degree of this extension in *mer*-$[Rh(dpt)_2]^{3+}$ is lower than that in *mer*-$[Co(dpt)_2]^{3+}$. This seems to be due to a relaxation in the chelate rings arising from an elongation of the M–N bond length; the M–N length is about 0.1 Å longer in the rhodium(III) complex than in the cobalt(III) one. The lowering in the degree of extension is compatible with a discussion based on the spectroscopic properties described above.

***mer*-$[Ir(dien)_2](ClO_4)_3\cdot 2H_2O$:** In this crystal, an iridium atom lies on a two-fold axis. Two dien ligands, which are related by the two-fold axis, coordinate by six nitrogen atoms to form an octahedral complex (Fig. 8). The complex has the *mer* configuration; a pair of two fused chelate rings has the (δλ, λδ) conformation. In addition to *mer*-$[Rh(dpt)_2]Cl(ClO_4)_2$, there exist two enantiomeric pairs (*trans*-δ-NH, and *trans*-λ-NH) in a unit cell. The N_6 octahedron is distorted compared with that in rhodium(III) or cobalt(III) complexes. As shown in Table 8, the difference between the longer (2.18(4) Å) and shorter (2.06(4) and 2.02(4) Å) M–N bond lengths can be regarded as being significant. Moreover, the N–M–N bond angles, especially those involving two terminal N atoms in a coordinated dien (N(1)–Ir–N(3)=167(2)°), are diminished from the ideal coordinating angle (180°). Such a situation leads to a rather distorted octahedron.

Geometry of dien or dpt Complexes: The calculated total energies $E_{\text{total}}/\text{kJ mol}^{-1}$) are plotted against the M–N bond lengths (l/Å) in Figs. 9 and 10. Figure 9 shows the energy minimum at ca. 2.05 Å in each geometrical isomer of the $[M(dien)_2]^{3+}$ complex. This result is comparable with the M–N bond length determined by an X-ray analysis for the *sym-fac*-$[Rh(dien)_2]Br_3$ crystal (mean Rh–N=2.07(1) Å). This also means that the Rh^{3+} ion has a best-fit size to form the $[M(dien)_2]^{3+}$ complex. Figure 9 also shows that

Table 7. Bond Distances and Angles within *mer*-$[Rh(dpt)_2]^{3+}$

Bond distance	l/Å	Bond angle	ϕ/°
Rh–N(1)	2.088(4)	N(1)–Rh–N(2)	91.75(14)
Rh–N(2)	2.118(4)	N(1)–Rh–N(3)	174.34(14)
Rh–N(3)	2.108(4)	N(1)–Rh–N(4)	92.57(14)
Rh–N(4)	2.087(4)	N(1)–Rh–N(5)	88.13(14)
Rh–N(5)	2.122(4)	N(1)–Rh–N(6)	91.46(15)
Rh–N(6)	2.110(4)	N(2)–Rh–N(3)	93.91(14)
		N(2)–Rh–N(4)	89.14(14)
N(1)–C(1)	1.483(6)	N(2)–Rh–N(5)	177.53(14)
N(2)–C(3)	1.499(6)	N(2)–Rh–N(6)	86.37(15)
N(2)–C(4)	1.498(6)	N(3)–Rh–N(4)	87.56(14)
N(3)–C(6)	1.488(6)	N(3)–Rh–N(5)	86.21(14)
N(4)–C(7)	1.490(6)	N(3)–Rh–N(6)	88.86(15)
N(5)–C(9)	1.497(6)	N(4)–Rh–N(5)	93.32(14)
N(5)–C(10)	1.501(6)	N(4)–Rh–N(6)	174.06(15)
N(6)–C(12)	1.487(6)	N(5)–Rh–N(6)	91.17(15)
C(1)–C(2)	1.493(7)	Rh–N(1)–C(1)	120.1(3)
C(2)–C(3)	1.498(7)	Rh–N(2)–C(3)	118.5(3)
C(4)–C(5)	1.511(7)	Rh–N(2)–C(4)	117.1(3)
C(5)–C(6)	1.501(7)	Rh–N(3)–C(6)	123.4(3)
C(7)–C(8)	1.503(8)	Rh–N(4)–C(7)	120.4(3)
C(8)–C(9)	1.500(8)	Rh–N(5)–C(9)	117.7(3)
C(10)–C(11)	1.501(7)	Rh–N(5)–C(10)	116.9(3)
C(11)–C(12)	1.501(7)	Rh–N(6)–C(12)	122.8(3)
		N(1)–C(1)–C(2)	110.9(4)
		N(2)–C(3)–C(2)	116.0(4)
		N(2)–C(4)–C(5)	113.5(4)
		N(3)–C(6)–C(5)	112.8(4)
		N(4)–C(7)–C(8)	111.5(4)
		N(5)–C(9)–C(8)	115.3(4)
		N(5)–C(10)–C(11)	115.0(4)
		N(6)–C(12)–C(11)	111.1(4)
		C(1)–C(2)–C(3)	114.2(4)
		C(4)–C(5)–C(6)	113.6(4)
		C(5)–C(8)–C(9)	114.3(5)
		C(10)–C(11)–C(12)	113.5(4)

Table 8. Bond Distances and Angles within *mer*-$[Ir(dien)_2]^{3+}$

Bond distance	l/Å	Bond angle	ϕ/°
Ir–N(1)	2.18(4)	N(1)–Ir–N(2)	81.7(14)
Ir–N(2)	2.06(4)	N(1)–Ir–N(3)	166.6(15)
Ir–N(3)	2.02(4)	N(2)–Ir–N(3)	85.0(15)
N(1)–C(1)	1.58(6)	Ir–N(1)–C(1)	105(2)
N(2)–C(2)	1.47(5)	Ir–N(2)–C(2)	108(2)
N(2)–C(3)	1.62(6)	Ir–N(2)–C(3)	102(3)
N(3)–C(4)	1.52(6)	Ir–N(3)–C(4)	109(3)
C(1)–C(2)	1.42(5)	C(2)–N(2)–C(3)	116(3)
C(3)–C(4)	1.52(6)	N(1)–C(1)–C(2)	109(3)
		N(2)–C(2)–C(1)	108(3)
		N(2)–C(3)–C(4)	105(4)
		N(3)–C(4)–C(3)	112(4)

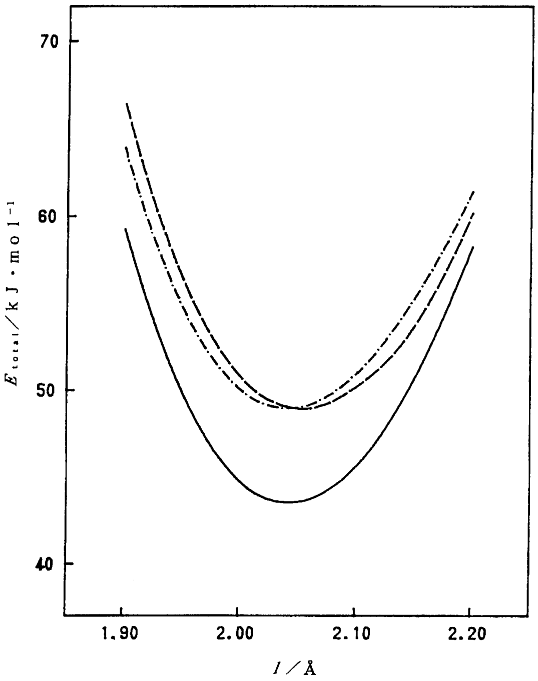

Fig. 9. Calculated total energy against the M–N bond lengths. —·—: *sym-fac*-$[M(dien)_2]^{3+}$, - - -: *unsym-fac*-$[M(dien)_2]^{3+}$, —: *mer*-$[M(dine)_2]^{3+}$.

the total energies of the isomers of $[M(dien)_2]^{3+}$ are *mer* (43.9)<*unsym-fac* (49.0)≒*sym-fac* (49.3 kJ mol^{-1}) for Rh–N (2.07 Å), and *mer* (47.4)<*sym-fac* (52.8)<*unsym-fac* (53.7 kJ mol^{-1}) for Co–N (1.97 Å).3—5) The yields of the isomers from the reacting mixture of the complex were *mer*>*unsym-fac*>*sym-fac* in the order for both of $[Rh(dien)_2]^{3+}$ (56>34>10%) and $[Co(dien)_2]^{3+}$ (e.g. 65>28>7%).6) The relations in the total energies among the isomers is not compatible with that in the experimental yields in respect to the order between *unsym-fac* and *sym-fac*. That is, the calculated results, that the energies for *unsym-fac* are nearly equal to or higher than that for *sym-fac*, are to be expected since the yields of *unsym-fac* are lower than that of *sym-fac*. However, the entropy effect (*unsym-fac* and *mer* isomers are dissymmetric) gives a 2:1 preference over the centrosymmetric *sym-fac*. Moreover, Yoshikawa has reported8) that a similar incompatibility between his calculated strain energies for the free $[Co(dien)_2]^{3+}$ ion and the yields of the isomers was elucidated based on his calculation, considering the formation of an ion pair of the complex cation and the counter ion. The results of the calculation showed that the *unsym-fac* isomer was more stabilized by forming a 1:1 ion pair with the Cl^- ion. These two factors seem to have a tendency to increase the formation of *unsym-fac*, but to decrease that of *sym-fac*. Considering this prediction, the present calculated results are compatible with the experimental ones for both cases of $[Rh(dien)_2]^{3+}$ and $[Co(dien)_2]^{3+}$. It is difficult to compute the formation energies for the present complexes, since the force constants for rhodium(III), which are comparable with those for cobalt(III), are not know. However,

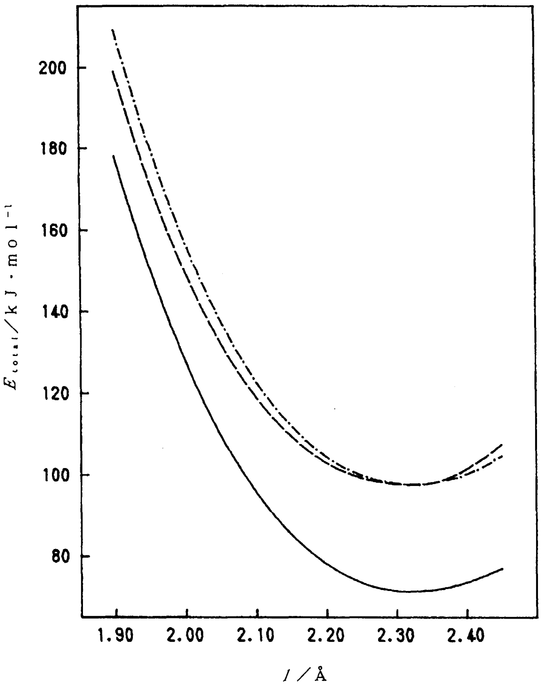

Fig. 10. Calculated total energy against the M–N bond lengths. –•–: *sym-fac*-$[M(dpt)_2]^{3+}$, ---: *unsym-fac*-$[M(dpt)_2]^{3+}$, —: *mer*-$[M(dpt)_2]^{3+}$.

the relations of the differences in the total energies between the *fac*-isomers and the *mer*-isomer ($E_{unsym\text{-}fac}-E_{mer}=5.1$ kJ mol^{-1} for $[Rh(dien)_2]^{3+}$, 6.3 kJ mol^{-1} for $[Co(dien)_2]^{3+}$: $E_{sym\text{-}fac}-E_{mer}=5.4$ kJ mol^{-1} for both the complexes) correspond to the yields of the isomers in both complexes. That is, the relations reproduce the tendency to increase the relative yields of the *fac*-isomers (in particularly *unsym-fac*) more in the $[Rh(dien)_2]^{3+}$ complex than in the $[Co(dien)_2]^{3+}$ complex.

Figure 10 shows the energy minimum at ca. 2.35 Å in each geometrical isomer of the $[M(dpt)_2]^{3+}$ complex. The total energy at 2.10 Å (Rh–N) decreases more than that at 2.00 Å$^{3-5)}$ (Co–N) in Fig. 10. However, the bond length, which corresponds to Rh–N (still more to Co–N) is too short to form a complex with the best-fit size. The short M–N length seems to cause a structural crowdedness to the two-fused six-membered chelate rings in the complex. This crowdedness leads to extended N–M–N angles, as observe in the results of an X-ray crystal analysis. Distinct from the $[M(dien)_2]^{3+}$ complex, the total energies of the *fac*-isomers in the $[M(dpt)_2]^{3+}$ complex are considerably higher (ca. 22 kJ mol^{-1} or above) than that of the *mer*-isomer. The fact that no *fac*-isomers were obtained in both complexes of rhodium(III) and cobalt(III), is explicable from the large difference in the energy.$^{34)}$

The experimental results in the yield of the isomers of the $[Ir(dien)_2]^{3+}$ complex (*mer*≫*unsym-fac*, *sym-fac*) and the failure to be prepare any isomers of $[Ir(dpt)_2]^{3+}$ are not explicable from the present molecular mechanics calculation. Unfortunately, it is difficult to estimate the force field which could lead to a reproduction of the distorted structure observed in the *mer*-$[Ir(dien)_2](ClO_4)_3 \cdot 2H_2O$ crystal, since very few structures have been reported concerning amine complex of iridium(III). At any rate the distorted structure suggests that the isomerism of the iridium(III) complexes can not be comparable with that of the cobalt(III) or rhodium(III) complexes.

The author is indebted to Professor Masayoshi Nakahara of Rikkyo University for his many helpful discussions.

References

1) F. G. Mann, *J. Chem. Soc.*, **1934**, 466.

2) Y. Yoshikawa and K. Yamasaki, *Bull. Chem. Soc. Jpn.*, **45**, 179 (1972).

3) M. Kobayashi, F. Marumo, and Y. Saito, *Acta Crystallogr., Sect. B*, **28**, 470 (1972).

4) M. Konno, F. Marumo, and Y. Saito, *Acta Crystallogr., Sect. B*, **29**, 739 (1973).

5) K. Okiyama, S. Sato, and Y. Saito, *Acta Crystallogr., Sect. B*, **35**, 2389 (1979).

6) F. R. Keene and G. H. Searle, *Inorg. Chem*, **13**, 2173 (1974).

7) T. W. Hambley, *Inorg. Chem.*, **27**, 2496 (1988).

8) Y. Yoshikawa, *J. Comput. Chem.*, **11**, 326 (1990), and references cited therein.

9) G. W. Watt and B. J. McCormick, *Inorg. Chem.*, **4**, 143 (1965).

10) T. W. Hambley, G. H. Searle, and M. R. Snow, *Aust. J. Chem.*, **35**, 1285, 1297 (1982).

11) S. Yamada, M. Umehara, M. Ishii, and M. Nakahara, *Nippon Kagaku Kaishi*, **1983**, 1733.

12) M. Ishii, M. Umehara, K. Harada, and M. Nakahara, *Bull. Chem. Soc. Jpn.*, **60**, 2683 (1987).

13) G. J. McDougall and R. D. Hancock, *J. Chem. Soc., Dalton Trans.*, **1980**, 654.

14) A. C. T. North, D. C. Phillips, and F. S. Mathews, *Acta Crystallogr., Sect. A*, **24**, 351 (1968).

15) "International Tables for X-Ray Crystallography," Kynoch Press, Birmingham (1974), Vol. IV, pp. 73, 75, 80, 83, and 92.

16) R. F. Stewart, E. R. Davidson, and W. T. Simpson, *J. Chem. Phys.*, **42**, 3175 (1965).

17) T. Sakurai and K. Kobayashi, *Rikagaku Kenkyusho Hokoku*, **55**, 69 (1978).

18) P. Main, M. M. Woolfson, and G. Germain, "MULTAN," Univ. of York, York, England and Univ. de Louvain, Louvain, Belgium (1971).

19) C. K. Johnson, "ORTEP, Report ORNL-3794," Oak Ridge National Laboratory, Tennessee (1965).

20) N. L. Allinger and Y. H. Yuh, *QCPE*, **12**, 395 (1980).

21) "3D-MOL Kaisetusyo (in Japanese)," Toray System Center, Tokyo (1990).

22) R. A. Bauer and F. Basolo, *Inorg. Chem.*, **8**, 2231 (1969).

23) C. K. Poon, T. W. Tang, and C. M. Che, *J. Chem. Soc., Dalton Trans.*, **1983**, 1647.

24) C. K. Jørgensen, "Absorption Spectra and Chemical

Bonding in Complexes," Pergamon Press, Oxford (1962), p. 109.

25) A. P. B. Lever, "Inorganic Electronic Spectroscopy," 2nd ed, Elsevier, Amsterdam (1984), pp. 463—466.

26) C. K. Jørgensen, *Adv. Chem. Phys.*, **5**, 33 (1963).

27) H. H. Schmidtke, *Z. Phys. Chem. (NF)*, **40**, 96 (1964).

28) H. H. Schmidtke, *J. Mol. Spectrosc.*, **11**, 483 (1963).

29) H. H. Schmidtke and D. Garthoff, *Inorg. Chim. Acta*, **1968**, 357.

30) A. Whuler, C. Brouty, and P. Herpin, *Acta Crystallogr., Sect. B*, **32**, 2238 (1976).

31) K. Yoshida, T. Kitada, N. Odano, M. Kashiwagi, K. Harada, A. Urushiyama, and M. Nakahara, *Bull. Chem. Soc. Jpn.*, **64**, 895 (1991).

32) K. Harada, K. Komiya, Y. Miyake, S. Harada, H. Saitoh, M. Umehara, and M. Nakahara, *Nippon Kagaku Kaishi*, submitted.

33) N. Odano, K. Harada, A. Urushiyama, and M. Nakahara, *Bull. Chem. Soc. Jpn.*, in press.

34) Hambley, et al. reported in Ref. 10 that the yield of the isomers of $[\mathrm{Co(dpt)_2}]^{3+}$ estimated from their molecular mechanics calculation is 99.3% for *mer*, 0.6% for *unsym-fac*, and 0.04% for *sym-fac* isomer, respectively. They also reported that the amount of the *sym-fac* isomer is predicted to be negligible, while the *unsym-fac* isomer is below the limit of chromatographic detection.